

# Physics based Modeling and Prognostics of Electrolytic Capacitors

Chetan S. Kulkarni \*

*Institute for Software Integrated Systems (ISIS), Vanderbilt University, Nashville, TN, 37235*

José R. Celaya †

*SGT Inc., NASA Ames Research Center, Moffett Field, CA, 94035*

Gautam Biswas ‡

*Institute for Software Integrated Systems (ISIS), Vanderbilt University, Nashville, TN, 37235*

Kai Goebel §

*NASA Ames Research Center, Moffett Field, CA, 94035*

**This paper proposes first principles based modeling and prognostics approach for electrolytic capacitors. Electrolytic capacitors and MOSFETs are the two major components, which cause degradations and failures in DC-DC converters. This type of capacitors are known for its low reliability and frequent breakdown on critical systems like power supplies of avionics equipment and electrical drivers of electro-mechanical actuators. Some of the more prevalent fault effects, such as a ripple voltage surge at the power supply output can cause glitches in the GPS position and velocity output, and this, in turn, if not corrected will propagate and distort the navigation solution. Prognostics provides a way to assess remaining useful life of a capacitor based on its current state of health and its anticipated future usage and operational conditions. In this paper, we study the effects of accelerated aging due to thermal stress on sets of capacitors. Our focus is on deriving first principles degradation models for thermal stress conditions. The degradation data form the basis for developing the model based remaining life prediction algorithm. Our overall goal is to derive accurate models of capacitor degradation, and use them to predict performance changes in DC-DC converters.**

## Nomenclature

$\epsilon_R$	relative dielectric constant
$\epsilon_O$	permittivity of free space
$V$	dispersion volume at time $t$
$V_O$	initial electrolyte volume
$j_{eo}$	evaporation rate ( $\text{mg min}^{-1} \text{ area}^{-1}$ )
$t$	time in hours
$\rho_E$	electrolyte resistivity
$P_E$	correlation factor related to electrolyte spacer porosity and average liquid pathway.
$w_e$	volume of ethyl glycol molecule
$V_c$	total capacitor capsule volume
$d_C$	thickness of cathode strip
$C$	Capacitance

---

\*Graduate Research Assistant, Institute for Software Integrated Systems

†Research Scientist, Prognostics Center of Excellence and AIAA Member.

‡Professor, Electrical Engineering and Computer Science, Institute for Software Integrated Systems

§Co-ordinator, Prognostics Center of Excellence and AIAA Member.

# I. Introduction

Most devices and systems today contain embedded electronic modules for monitoring, control and enhanced functionality. However, it has been found that these modules are often the first elements in the system to fail thus reducing overall system reliability.<sup>1-3</sup> These failures can be attributed to adverse operating conditions, such as high temperatures, voltage surges and current spikes.

Avionics systems play a critical role in many aspects of aircraft flight control. As the system complexity and flight criticality of functions performed by these systems increases, the related consequences of in-flight malfunctions are bound to increase. This drives the need for Integrated Vehicle Health Management (IVHM) technologies for flight-critical avionics. Studying and analyzing the performance degradation of embedded electronics in the aircraft domain is absolutely necessary to increase aircraft reliability, assure in-flight performance, and reduce maintenance costs.<sup>3,4</sup> In addition to this, an understanding of the behavior of deteriorated components is needed as well as the capability to anticipate failures and predict the remaining useful life (RUL) of the electronic systems.

The term “diagnostics” relates to the ability to detect and isolate faults or failures in a system. “Prognostics” on the other hand is the process of predicting health condition and remaining useful life based on current state and previous, current and future operating conditions. Prognostics and health management (PHM) methods combine sensing, data collection, interpretation of environmental, operational, and performance related parameters to indicate systems health as well as anticipate damage propagation due to degradation. PHM methodologies can be implemented through the use of various techniques that study parameter variations, which indicate changes in performance degradation based on usage duration and conditions.

## A. Background

An avionics system module consists of hardware (power supply, Global positioning system (GPS) receiver, Inertial measurement unit (IMU)) and software (GPS software, INAV - integrated navigation solution) components. Switched-mode power supplies are widely used in DC-DC converters because of their high efficiency and compact size. The buck-boost DC-DC converter steps voltage levels down/up based on the application requirements. Our particular application has an input of 28V DC from a battery source, and the required output voltage of 5V. The schematic of this system is shown in Fig. 1. The electrolytic capacitors and metaloxidesemiconductor field-effect transistor (MOSFET) switches are known to have the highest degradation and failure rates among all of the components.<sup>5</sup> Degraded capacitors affect the performance and efficiency of the DC-DC converters in a significant manner and also impose a risk on instantiating cascading failures on other connected subsystems.

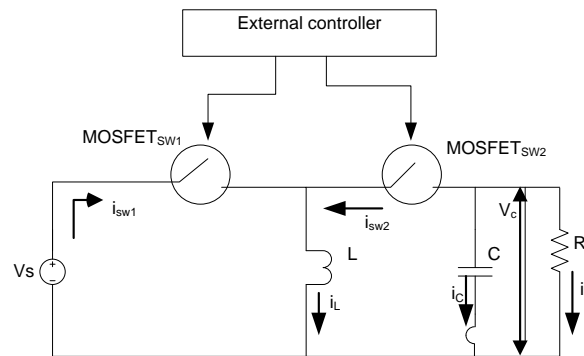


Figure 1. Buck-boost Converter Circuit

Some of earlier efforts in diagnostic health monitoring of electronic systems and subsystems involved the use of a built-in test (BIT), defined as an on-board hardware-software diagnostic tests to identify and locate faults. Studies conducted by<sup>6,7</sup> on the use of BITs for fault identification and diagnostics showed that they can be prone to false alarms and may result in unnecessary costly replacement, re-qualification, delayed shipping, and loss of system availability. The persistence of such issues over the years is perhaps because the use of BIT has been restricted to low-volume systems. In general, BITs generally have not been designed to provide prognostics or remaining useful life due to accumulated damage or progression of faults. Rather, it has served primarily as a diagnostic tool.

Degradation in electronics is more difficult to detect and inspect, due to difficulty in physics based modeling and the complex architecture of most electronic products.<sup>1</sup> Prognostics failure predictions have to be accurate if they are used in taking decisions for reliability improvement and repair. Detailed examinations of actual parameter variations and degradation process should also be compared with those that are predicted by the physics-based failures models. Between similar components or electronic systems, but made by different manufacturers, there may be wide variability in the parameters values and hence making effective predictions based on specific data set.<sup>8</sup> Hence implementing PHM methodology based on first principles of operation is highly effective and efficient in making remaining useful life predictions under such circumstances.

In this paper we develop an effective PHM methodology that applies to electronic systems and components. In particular, we develop a methodology for modeling to enable early detection of failure precursors in capacitor elements associated with DC-DC power supplies. Our approach combines physics-based modeling supported by empirical experimental analysis for deriving the degradation models, and then using these models to predict remaining useful life of electrolytic capacitors as well as their effects on overall system performance. Our hypothesis is that early detection will lead to better prediction and end of life estimates by tracking and modeling the degradation process.

## **B. Organization of Paper**

This paper is organized as follows. Section II discusses the current work being done in the area of capacitor prognostics and our research approach. Section III presents introduction to electrolytic capacitors and its basic structure, operation and degradation mechanisms. Section IV discusses capacitor first principle models in detail. Section V describes the thermal stress aging experiments conducted for this work. Section VI and VII presents the prognostic framework methodology and RUL results respectively. The paper ends with discussion and conclusion in section VIII.

## **II. Related Work**

The output filter capacitor has been identified as one of the elements of a switched mode power supply that fails more frequently, and therefore, has a critical impact on performance.<sup>9-12</sup> A prognostics and health management (PHM) approach for power supplies of avionics systems is presented by Orsagh.<sup>12</sup> Results from accelerated aging of the power supply systems are discussed in terms of output capacitor and power MOSFET failures. However there is no discussion on degradation process or to make RUL predictions for the power supply. The work on switched mode power supplies by<sup>9,11</sup> look into the details of the power supply output ripple voltage and leakage current as a function of time and degradation of the capacitor. But lacks details related to modeling the degradation mechanisms and RUL prediction computations are not presented in detail.

The work by<sup>13</sup>, focuses on the temperature-humidity bias accelerated test to replicate failures for multilayer ceramic capacitors. Their approach uses data trending algorithms in conjunction with multivariate decision-making. The Mahalanobis distance is used to detect abnormalities within the data and classify the data into “normal” and “abnormal” groups. The abnormal data are then further classified into severity levels of abnormality based on which RUL predictions are done. In the study done by<sup>14</sup>, multi-layer ceramic capacitors were selected for in-situ monitoring and life testing under elevated temperature, humidity and voltage conditions. This method uses data from accelerated aging tests to detect potential failures and make an estimation of time of failure. A data driven fault detection and prediction algorithm for multilayer ceramic capacitors is presented by J. Gu<sup>15</sup>. The prediction approach used in this study combines regression analysis, residual, detection and prediction analysis. A method based on Mahalanobis distance is used to detect abnormalities in the test data; there is no prediction of RUL.

## **A. Research Approach**

We adopt a physics based modeling (PBM) approach to predict the dynamic behavior of the system under nominal and degraded conditions. Faults and degradations appear as parameter value changes in the model, and this provides the mechanisms for tracking system behavior under degraded conditions.<sup>16,17</sup>

In the research work we focus our study towards degradation/failures under stress in electrolytic capacitors derived from the first principles of operation. Identifying the failure precursors and developing accurate models of degradation/failure has been the most difficult problem of our research goal. These precursors includes parameters like ripple voltage, ripple current, leakage currents in the power supply system. Early detection and analysis may lead to better prediction and end of life estimates of the capacitor by tracking and modeling the degradation process.

Therefore, one of our goals is to use these estimates to make accurate and precise prediction of the time to failure of electrolytic capacitors and degradation of overall system performance. This is achieved through a physics of failure

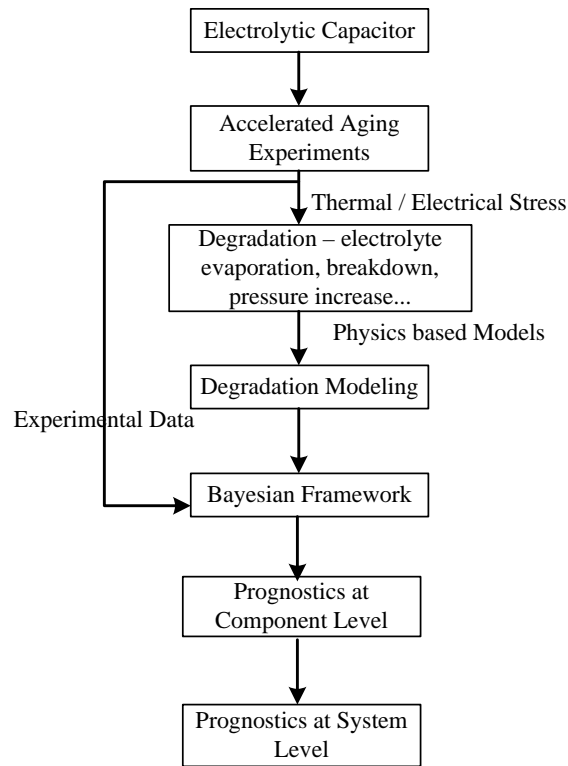


**Figure 2. Research Approach Methodology**

based approach by modeling capacitor degradation models under different operating conditions. Experimental studies are being conducted and first principles based physics models are being derived using the descriptions of capacitor degradation mentioned in literature,<sup>18–21</sup> and then deriving accurate physics based degradation models using our experimental data. Our second goal is to have the ability to predict DC-DC converter system performance as the capacitors degrade (not discussed in this paper). Our approach is summarized in Fig. 2. This figure outlines the steps needed to build the individual degradation models and propagate their effects to system level analysis.

In the next section we first discuss in brief the basics of electrolytic capacitors, their detailed structure and the different mechanisms under which the devices degrade.

### III. Electrolytic Capacitors

Electrolytic capacitor performance is strongly affected by its operating conditions, such as voltage, current, frequency, and ambient temperatures. A primary reason for wear out in aluminum electrolytic capacitors is due to vaporization of electrolyte and degradation of electrolyte due to ion exchange during charging/discharging, which in turn leads to a drift in the two main electrical parameters of the capacitor: (1) the equivalent series resistance (*ESR*), and (2) the capacitance (*C*). The *ESR* of a capacitor is the sum of the resistance due to aluminum oxide, electrolyte, spacer, and electrodes (foil, tabbing, leads, and ohmic contacts)<sup>19</sup> and capacitance is the ability of a capacitor to store charge in an electric field. The health of a capacitor is often measured by the values of these two parameters. There are certain industry standard thresholds for these parameter values, if the measurements exceed these thresholds then the component is considered unhealthy, i.e., the component has reached its end of life, and should be immediately replaced before further operations.<sup>22,23</sup>

An aluminum electrolytic capacitor, as illustrated in Fig. 3 an capacitor consists of a cathode aluminum foil, electrolytic paper, electrolyte, and an aluminum oxide layer on the anode foil surface, which acts as the dielectric. When in contact with the electrolyte, the oxide layer possesses an excellent forward direction insulation property.<sup>19</sup> Together with magnified effective surface area attained by etching the foil, a high capacitance value is obtained in a small volume.<sup>20</sup> Since the oxide layer has rectifying properties, a capacitor has polarity. If both the anode and cathode foils have an oxide layer, the capacitors would be bipolar.<sup>24</sup> In this work, we analyze “non-solid” aluminum

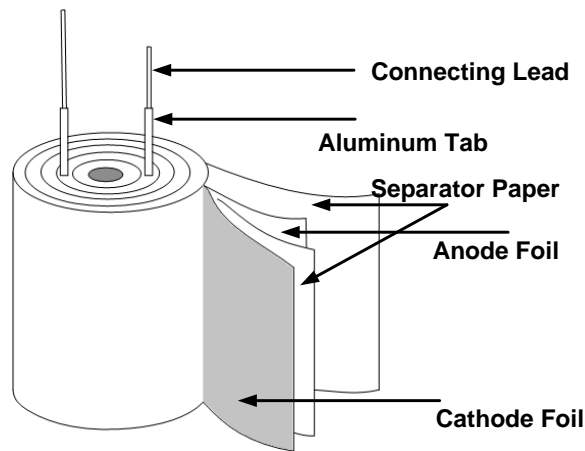


Figure 3. Physical Model of Electrolytic Capacitor

electrolytic capacitors in which the electrolytic paper is impregnated with liquid electrolyte. Another type of aluminum electrolytic capacitor that uses solid electrolyte<sup>25</sup> is not discussed in this work.

Fig. 4 shows a detailed view of the cross section of an electrolytic capacitor structure along with its equivalent electrical circuit diagram. To get higher capacitance values for the same surface area of the anode and cathode foils, the foil is etched by a chemical process. After etching, the plates are anodized by coating them with a thin aluminum oxide layer on the surface of the foil. This layer of aluminum oxide acts as the dielectric (insulator) and serves to block the flow of direct current between the two capacitor plates.<sup>18,20</sup>

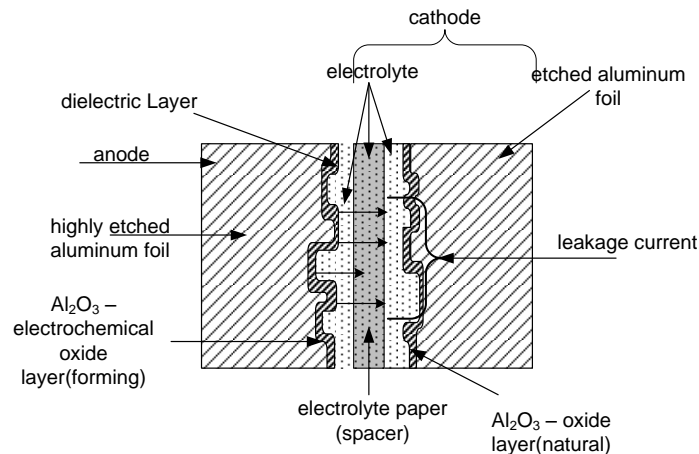


Figure 4. Capacitor Detail Structure

### A. Degradation Mechanisms

There are several factors that cause degradation in electrolytic capacitors. Failures in a capacitor can be one of two types: (1) catastrophic failures, where there is complete loss of functionality due to a short or open circuit, and (2) degradation failures, where there is gradual deterioration of capacitor due to accumulated damages. Degradation in the capacitor manifests an increase in the equivalent series resistance (*ESR*) and decrease in capacitance (*C*), due to deterioration of electrolyte quality, decreases in electrolyte volume due to evaporation, weakening of the oxide layer, over operating time.<sup>19,26</sup>

The flow of current during the charge/ discharge cycle of the capacitor causes the internal temperature to rise. The heat generated is transmitted from the core to the surface of the capacitor body, but not all the heat generated

can escape. The excess heat results in a rise in the internal temperature of the capacitors which causes the electrolyte to evaporate, and gradually deplete. Similarly in situations where the capacitor is operating under high temperature conditions, the capacitor body is at a higher temperature than its core, the heat travels in the opposite directions from the body surface to the core of the capacitor again increasing the internal temperature causing the electrolyte to evaporate. This is explained using a first principles thermal model of heat conduction.<sup>27</sup>

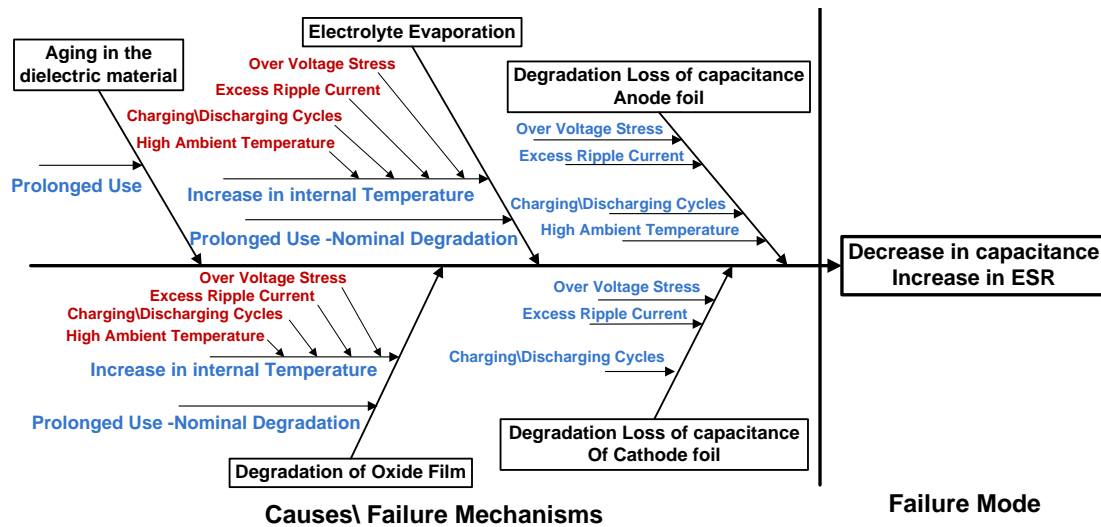


Figure 5. Fishbone diagram of failure mechanisms in aluminum electrolytic capacitor

Degradation in the oxide layer can be attributed to crystal defects that occur because of the periodic heating and cooling during the capacitor's duty cycle, as well as stress, cracks, and installation-related damage. High electrical stress is known to accentuate the degradation of the oxide layer due to localized dielectric breakdowns on the oxide layer.<sup>28</sup> These breakdowns, which accelerate the degradation, have been attributed to the duty cycle, i.e., the charge/discharge cycle during operation.<sup>19,29</sup> Further another simultaneous phenomenon is the increase in the internal pressure due to an increased rate of chemical reactions,<sup>19,29</sup> which can again be attributed to the internal temperature increase in the capacitor. This pressure increase can ultimately lead to the capacitor popping open at the top.

All the failure/degradation phenomenon mentioned may act simultaneously based on the operating conditions of the capacitors. We first study the phenomenon qualitatively, and then discuss the steps to derive the first principles analytic degradation models for the different operating condition. The fishbone diagram (also called the Ishikawa diagram) in Fig. 5 shows the most common set of failure modes for electrolytic capacitors that have been reported in the literature.<sup>19,29</sup> This diagram identifies the relationship between root causes and failure modes observed in electrolytic capacitors.

These root causes can occur individually or combined manner in a capacitor depending upon the conditions of operation. Our focus in this work is on the thermal stressors that govern the capacitor degradation, specifically, we study high temperature scenarios and their effects on the electrolytic capacitor degradation. The physics-of-failure approach uses the knowledge of component behavior under different operating conditions, and load conditions to identify potential failure. The approach is used to model the root causes of failure such as fatigue, fracture, wear, and corrosion.

#### IV. Physics based Modeling of Capacitor Degradation

Based on the above discussions on degradation and experiments conducted, in this section we discuss about deriving the first principles models for thermal overstress conditions. Under thermal overstress conditions since the device was subjected to only high temperature with no charge applied we observe degradation only due to electrolyte evaporation. The models are derived based on this observations and measurements see during from the experimental data.

## A. Structural Model

For deriving the physics based models it is also very much necessary to know about the structural details of the component under study. The models defined use this information for making effective degradation/failure predictions. A detail structural study of the electrolytic capacitor under test is discussed in this section.

During modeling it is not possible to know the exact amount of electrolyte present in a capacitor. But using information from the structure details we can approximately calculate the amount of electrolyte present. Based on the type and configuration, the electrolyte volume will vary which can be updated in the model parameters. The equation for calculating the approximate electrolyte volume is derived from calculating the volume of the total capacitor capsule,  $V_c$  given by :

$$V_c = \pi r_c^2 h_c \quad (1)$$

where :

$r_c$  = radius of capacitor capsule

$h_c$  = height of capacitor capsule

The approximate volume of electrolyte,  $V_e$  based on geometry of the capacitor is expressed in terms of following equation:

$$V_e = \pi r_c^2 h_c - A_{surface}(d_A + d_C) \quad (2)$$

where :

$A_{surface}$  = effective oxide surface area

$d_C$  = thickness of cathode strip,

$d_A$  = thickness of anode strip.

## B. Equivalent Electrical Circuits

A simplified electrical lumped parameter model of impedance,  $\mathcal{M}_1$ , defined for a electrolytic capacitor is shown in Fig.6. The ESR dissipates some of the stored energy in the capacitor. For a good capacitor operating nominally this current is not significant, but it becomes larger as the oxide layer degrades during operation. An ideal capacitor would offer no resistance to the flow of current at its leads. However, the electrolyte , aluminum oxide , space between the plates and the electrodes combined produces a small equivalent internal series resistance ( $ESR$ ).

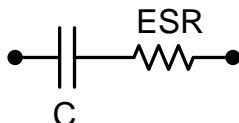


Figure 6. Lumped Parameter Model ( $\mathcal{M}_1$ )

From the literature<sup>25,30,31</sup> and experiments conducted under thermal overstress, it has been observed that the capacitance and ESR value depends of the electrolyte resistance  $R_E$ . A more detailed lumped parameter model derived for an electrolytic capacitor under thermal overstress condition,  $\mathcal{M}_2$  can be modified from  $\mathcal{M}_1$ , as shown in fig. 7.  $R_1$  is the combined series and parallel resistances in the model.  $R_E$  is the electrolyte resistance. The combined resistance of  $R_1$  and  $R_E$  is the equivalent series resistance of the capacitor.  $C$  is the total capacitance of the capacitor as discussed earlier.

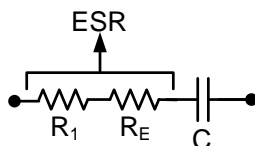


Figure 7. Lumped Parameter Model ( $\mathcal{M}_2$ )

### C. Electrolyte Decrease

Exposure of the capacitors to temperatures  $T_{applied} > T_{rated}$  results in accelerated aging of the devices<sup>18,32,33</sup>. Higher ambient storage temperature accelerates the rate of electrolyte evaporation leading to degradation of the capacitance.<sup>18,25</sup> The depletion in the volume and thus the effective surface area is given by :

$$V(t) = V_o - (A_{surface} j_{eo} w_e) \times t \quad (3)$$

Details of the derivation of this equation can be found in.<sup>30,32</sup>

### D. Capacitance Degradation Model

The input impedance of the capacitor network is defined in terms of the total lumped series and parallel impedance of the simplified network. The total lumped capacitance of the structure is given by

$$C = (2\epsilon_R\epsilon_0 A_{surface})/d_C \quad (4)$$

Thus from Eq. (3) and (4) we can derive the first principles capacitance degradation model,  $\mathcal{M}_3$  which is given by :

$$C(t) = \left[ \frac{2\epsilon_R\epsilon_0}{d_C} \right] \left[ \frac{V_o - V(t)}{j_{eo} t w_e} \right] \quad (5)$$

The degraation in capacitance is directly proportional to the damage variable  $V$ . As discussed earlier, increase in the core temperature evaporates the electrolyte thus decreasing the electrolyte volume leading to degradation in capacitance. The resultant decrease in the capacitance can be computed using Eq. (5).

## V. Thermal Overstress Experiment

In this setup we emulated conditions similar to high temperature storage conditions,<sup>18,32</sup> where capacitors are placed in a controlled chamber and the temperature is raised above their rated specification.<sup>33</sup> Pristine capacitors were taken from the same lot rated for 10V and maximum storage temperature of 85°C.

The chamber temperature was gradually increased in steps of 25°C till the pre-determined temperature limit was reached. The capacitors were allowed to settle at a set temperature for 15 min and then the next step increase was applied. This process was continued till the required temperature limit was attained. To decrease possibility of shocks due to sudden decrease in the temperature the above procedure was followed.

Experiments done with 2200  $\mu$ F capacitors with TOS temperature at 105°C and humidity factor at 3.4%. At the end of specific time interval the temperature was lowered in steps of 25°C till the required room temperature was reached. Before being characterized the capacitors were kept at room temperature for 15 min. The ESR value is the real impedance measured through the terminal software of the instrument. Similarly the capacitance value is computed from the imaginary impedance using Electrochemical Impedance Spectroscopy (EIS). Characterization of all the capacitors was done for measuring the impedance values using an SP-150 Biologic impedance measurement instrument.<sup>34</sup> Fig. 8 shows the plots decrease in capacitance due to accelerated aging for all the 15 capacitors under test at different aging times.

In the thermal overstress experiments, the capacitors we characterized periodically and after 3400 hours of operation it was observed that the average capacitance value decreased by more than 9-11% while decrease in the *ESR* value was observed around 20 - 22%. From literature<sup>33</sup> under thermal overstress conditons higher capaitance degradation is observed and minor degradation in ESR which correlated with the data collected. Hence the capacitance degradation data was used as a precursor to failure parameter to estimate the current health condition of the device.

## VI. Model-based Prognostics Framework

In our earlier work<sup>17,19,29</sup> an implementation of a model-based prognostics algorithm based on Kalman filter (KF) and a physics inspired empirical degradation model has been presented. The physics inspired degradation model was derived based on the capacitance degradation data from electrical overstress experiments. This model relates aging time to the percentage loss in capacitance and has the following form,

$$C(t) = e^{\alpha t} + \beta \quad (6)$$



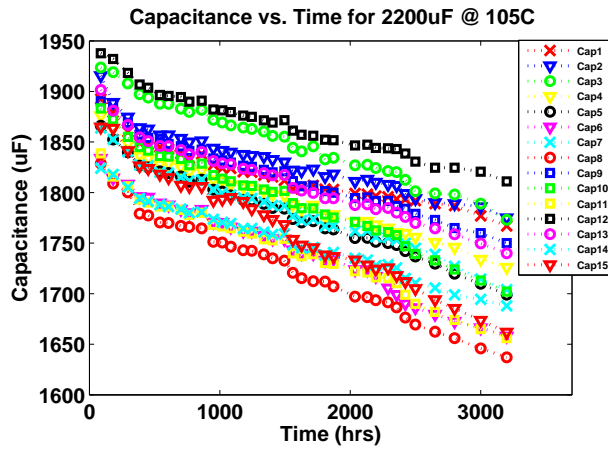


Figure 8. Capacitance Plot for all the devices under TOS

where model constants  $\alpha$  and  $\beta$  were estimated from the experimental data

Here the exponential model was linked to the degradation data and parameters were derived based on this data. The exponential empirical model derived in Eq. (6) was further updated and as discussed in section (D) we developed a first principles based generalized model to be implemented for different capacitor types and operating conditions.

In this section we present extension of our previous work<sup>17,19</sup>. A model-based prognostics algorithm based on Kalman filter and a physics inspired empirical degradation model is presented. The prognostic methodology implemented in this work consists two parts. The first part consists of a tracking framework where the algorithm tracks the state based on the current conditions of the device and inputs. In second part the algorithm is able to predict remaining useful life of the capacitor till the health threshold of the device is crossed.

### A. Dynamic Models

From section IV we have the physics model of capacitor given by Eq. (4):

From the structure of capacitor we have the electrolyte volume( $V_e$ ) expressed in the form of oxide surface area ( $A_{surface}$ ) as :

$$\begin{aligned} V_e &= A_{surface} \cdot d_C, \\ A_{surface} &= \frac{V_e}{d_C}. \end{aligned} \quad (7)$$

substituting from the Eq. (7) we have:

$$C(t) = \left[ \frac{2\epsilon_R \epsilon_0}{d_C} \right] \left[ \frac{V_e}{d_C} \right] \quad (8)$$

From Eq. (3) the first order discrete approximation for change in electrolyte volume can be expressed as:

$$\begin{aligned} \frac{dV}{dt} &= -(w_e A_{surface} j_{eo}), \\ V_{k+1} &= V_k + \frac{dV}{dt} \Delta t, \\ V_{k+1} &= V_k - (w_e A_{surface} j_{eo}) \Delta t. \end{aligned} \quad (9)$$

from Eq. (8) we have,

$$\begin{aligned} V_k &= \frac{C_k}{2\epsilon_R \epsilon_0} d_C^2, \\ V_k &= (C_k) \alpha. \end{aligned} \quad (10)$$

where:

$$\alpha = \frac{d_C^2}{2\epsilon_R\epsilon_0}$$

Now;

$$C_{k+1} = C_k + \frac{dC}{dt}\Delta t, \quad (11)$$

From Eq. (10) we can express Eq. (9) as :

$$\begin{aligned} C_{k+1}\alpha &= C_k\alpha + \frac{dC}{dt}\Delta t, \\ C_{k+1}\alpha &= C_k\alpha - (w_e A_{surface} j_{eo})\Delta t, \text{ hence} \\ C_{k+1} &= C_k - \frac{(w_e A_{surface} j_{eo})}{\alpha}\Delta t. \end{aligned} \quad (12)$$

The complete discrete time dynamic model for capacitance degradation can be summarized as :

$$\mathcal{M}_3 : C_{k+1} = C_k - \frac{(2\epsilon_R\epsilon_0 w_e A_{surface} j_{eo})}{d_C^2}\Delta t \quad (13)$$

The model  $\mathcal{M}_3$ , in Eq. (13) is implemented in a bayesian tracking framework. In this work we are implementing a Kalman Filter (K.F) since the degradation in capacitance (state) due to decrease in electrolyte is considered to be a dynamic linear model due to the assumption of constant evaporation rate ( $j_{eo}$ ) under constant thermal stress conditions. Next we discuss the implementation of the bayesian framework methodology for prognostics<sup>35-37</sup>.

1. State tracking (Kalman Filter): The current measured capacitance ( $C$ ) is defined as the state variable to be estimated and the degradation model is expressed as a discrete time dynamic model in order to estimate current capacitance ( $C$ ) due to decrease in electrolyte volume at the next available measurement. Direct measurements of the capacitance ( $C$ ) are assumed for the filter.
2. Health state forecasting: It is necessary to forecast the state variable once there are no more measurements available at the end of step 1. This is done by evaluating the degradation model through time using the state estimate at time  $t$  as initial value.
3. Remaining useful life computation: RUL is computed as the time between time of prediction  $t$  and the time at which the forecasted state crosses the failure threshold value.

These steps are repeated for different aging time ( $t_p$ ) through the life of the capacitor device under test.

## B. Kalman filter for state estimation

A state-space dynamic model is needed for filtering. The state variable  $x_k$  (Capacitance) at time  $t_k$  is defined as the current measured capacitance  $C_k$ . Since the system measurements are capacitance ( $C$ ) as well, the output equation is given by  $y_k = D_k$ , where the value of  $D$  is equal to one. The following system structure is implemented for filtering and prediction using a Kalman Filter.

$$\begin{aligned} x_k &= A_k x_{k-1} + B_k u + v, \\ y_k &= D_k + w. \end{aligned} \quad (14)$$

where,

$$\begin{aligned} A &= 1, \\ B &= -\frac{(2\epsilon_R\epsilon_0 w_e A_{surface} j_{eo})}{d_C^2}\Delta t, \\ D &= 1, \\ u &= j_{eo}. \end{aligned} \quad (15)$$

In this work and application of KF, the time increment between measurements  $\Delta t$  is not constant since measurements were taken at nonuniform time intervals i.e., the capacitors were characterized at different time intervals. This implies that some of the parameters of the model in Eqn. (14) will change through time. Furthermore,  $v$  and  $w$  are normal random variables with zero mean and  $Q$  and  $R$  variance respectively. The model noise (process noise) variance  $Q$  was estimated from the model regression residuals and was used for the model noise in the Kalman filter implementation. The measurement noise variance  $R$ , was computed from the direct measurements of the capacitance with the EIS equipment, the observed variance is  $4.99 \times 10^{-7}$ . A detailed description of the KF algorithm implemented in this work can be found in <sup>38</sup>, a description of how the algorithm is used for forecasting can be found in <sup>39</sup> and an example of its usage for prognostics can be found in <sup>35,36</sup>.

### C. Future state forecasting

The use of the Kalman filter for state estimation as a RUL forecasting algorithm requires the evolution of the state without updating the error covariance matrix and the posterior of the state vector.  $A$  and  $B$  are the matrices for a linear system implemented. The  $n$  step ahead forecasting equation for the Kalman filter is given below. The last update is done at the time of the last measurement  $t_l$ .

$$\hat{x}_{l+n} = A^n x_l + \sum_{i=0}^{n-1} A^i B \quad (16)$$

The subscripts from parameters  $A$  and  $B$  are omitted since a constant  $\Delta t$  is used in the forecasting mode (one prediction every hour).

## VII. Prediction of Remaining Useful Life Results

State estimation and RUL prediction results are discussed for capacitor Cap # 5. Figure 9 out of a batch of 15 available capacitors under test, shows the result of the filter tracking for completed degradation in capacitance upto 3200 hours of aging time. The residuals show an increased error with aging time, since we have implemented degradation due to a constant evaporation rate under thermal overstress condition and the breakdown in the oxide layer due to stress is not considered for this model which starts to dominate in the later stages of aging of the device. This breakdown is exponential in nature and as we can observe a dip in the capacitance values from the linear path in the later stages.

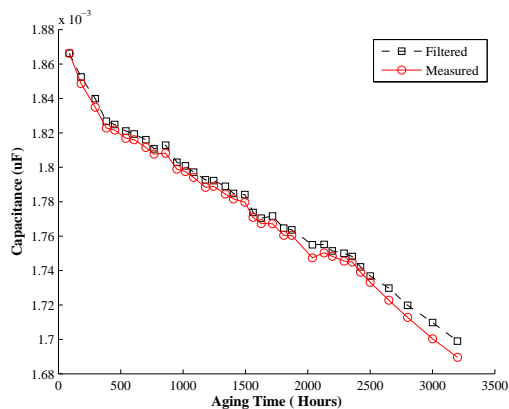


Figure 9. Tracking filter output against measurement data for Cap # 5

Figure 10 presents results from the remaining useful life prediction algorithm at different aging times  $t_p = 87.5, 607, 1495, 2131, 2800$  (hrs), at which the capacitors are characterized and their capacitance ( $C$ ) value is calculated. The failure threshold is considered to be 10% decrease in capacitance value, which in this case is at 3200 hours of aging time. End of life (EOL) is defined as the time at which the forecasted capacitance value trajectory crosses the EOL threshold. Therefore, RUL is EOL minus aging times  $t_p = 87.5, 607, 1495, 2131, 2800$  (hrs).

An  $\alpha$ - $\lambda$  prognostics performance metric<sup>40,41</sup> is presented in figure 11 for test case of Cap #5. Performance metric identifies whether the algorithm performs within desired error margins (specified by the parameter  $\alpha$ ) of the actual

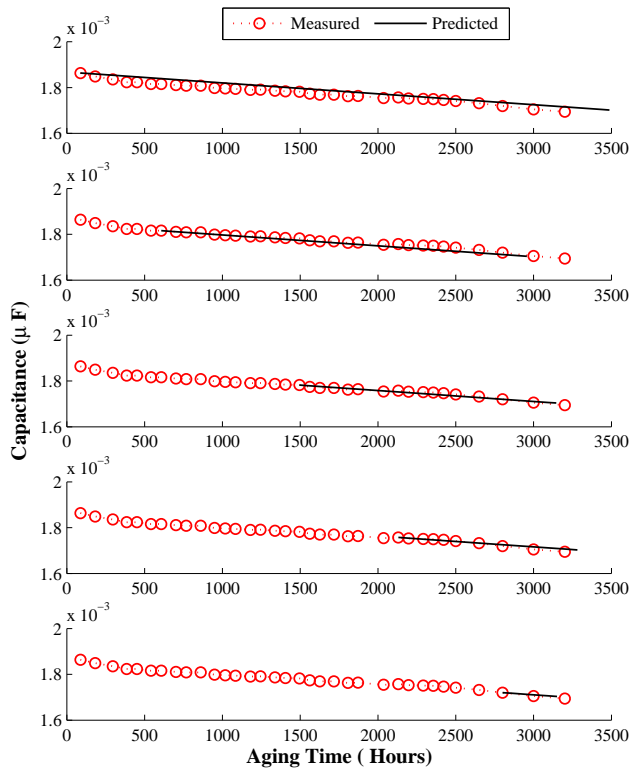


Figure 10. Capacitance decrease prediction at different Aging Time for Cap # 5

RUL at any given time instant (specified by the parameter  $\lambda$ )<sup>40</sup>. The central dashed line represents ground truth and the shaded region is corresponding to a 10% ( $\alpha = 0.1$ ) error bound in the RUL prediction.

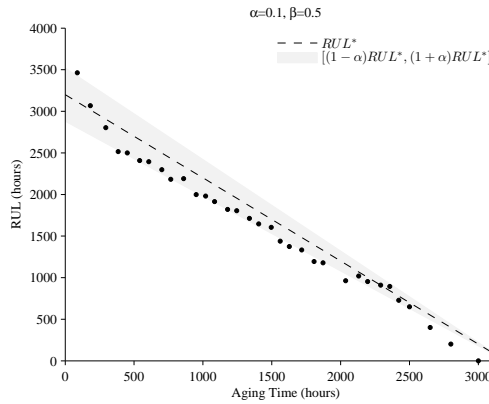


Figure 11. Performance based on Alpha-Lambda metric for Cap#5

From the  $\alpha$ - $\lambda$  metric plot in Fig. 11 it can be observed that the relative accuracy is not as good at the end but the accuracy is good enough under acceptable limits. This is due to the non-linearity observed in the data at the end of the aging time. It can be seen that most of the points satisfy the performance metrics and the noise observed in the central part is mainly due to the correction action taken. Other wise we would have observed a biased straight line in case no correction action was applied to the data by the filter.

## VIII. Conclusion and Discussion

This paper presents a first principles based degradation electrolytic capacitor model and an parameter estimation algorithm to validate the derived model, based on the experimental data. The majors contributions of the work presented in this paper are:

1. Development of the first principles degradation model based on accelerated life test aging data which includes decrease in capacitance as a function of time and evaporation rate linked to temperature conditions;
2. Implementation of a Bayesian based health state tracking and remaining useful life prediction (RUL) algorithm based on the Kalman filtering framework.
3. Prediction of remaining useful life for capacitors based first principles degradation model,  $\mathcal{M}_3$ .

The degradation model,  $\mathcal{M}_3$  based on the first principles gives an indication of how a specific device degrades based on its structure, material properties, operating conditions, etc. The derived model can be updated and developed at a finer granular level to be implemented for detailed prognostic implementation. The results presented here are based on accelerated aging experimental data and on the accelerated life timescale. In our earlier work we studied the degradation models based on the observed data, and the work discussed here is a next step to generalize the model. Though as discussed in section IV, as a first step a dynamic linear model has been implemented for degradation model. This degradation model for decrease in capacitance,  $C$  due to an assumed constant evaporation rate  $\dot{j}_{eo}$  needs to be updated and include the model of break-down in the oxide layer which is exponential in nature and dominates in the later stages of aging. Further research will focus on development of functional mappings that will translate the accelerated life timescale into real usage conditions timescale, where the degradation process dynamics will be slower, and subjected to varying stress conditions.

The performance of the proposed first principles degradation model,  $\mathcal{M}_3$  is acceptable for the current study based on the quality of the model fit to the experimental data and the RUL prediction performance from  $\alpha$ - $\lambda$  metric plot. Additional experiments are currently underway to increase the number of test samples. This will greatly enhance the quality of the model, and guide the exploration of additional degradation-models, where the loading conditions and the environmental conditions are also accounted for towards degradation dynamics.

## References

- <sup>1</sup>Vichare, N. and Pecht, M., "Prognostics and Health Management of Electronics," *IEEE Transactions on Components and Packaging Technologies*, Vol. Vol 29, 2006, pp. 222 – 229.
- <sup>2</sup>FIDESGroup, "Reliability Methodology for Electronic Systems," *FIDES Guide issue A*, 2004.
- <sup>3</sup>Ferrell, B. L., "JSF Prognostics and Health Management," *IEEE Aerospace Conference*, 1999, pp. 471.
- <sup>4</sup>Celaya, J. R., Wysocki, P., Vashchenko, V., Saha, S., and Goebel, K., "Accelerated aging system for prognostics of power semiconductor devices," *IEEE AUTOTESTCON, 2010*, Orlando, FL, 2010, pp. 1–6.
- <sup>5</sup>Goodman, D. and et'al, "Practical Application of PHM/Prognostics to COTS Power Converters," *Aerospace Conference, 2005 IEEE*, March 2005, pp. 3573–3578.
- <sup>6</sup>Pecht, M., Dube, M., Natishan, M., and Knowles, I., "An Evaluation of Built-In Test," *IEEE Transactions on Aerospace and Electronic Systems*, Vol. 37, January 2001, pp. 266–272.
- <sup>7</sup>Johnson, D., "Review of Fault Management Techniques Used in Safety Critical Avionic Systems," *Progress in Aerospace Science*, Vol. 31, October 1996, pp. 415–431.
- <sup>8</sup>Leonard, C. and Pecht, M. G., "Improved techniques for cost effective electronics," *Proc. Reliability Maintainability Symp*, 1991, pp. 174 – 182.
- <sup>9</sup>Judkins, J. B., J. H., and S. V., "A Prognostic Sensor for Voltage Regulated Switch-Mode Power Supplies," *IEEE Aerospace Conference*, Vol. 1, No. 10.1109/AERO.2007.352885, 2007, pp. 1–8.
- <sup>10</sup>Vohnout, S., Kozak, M., Goodman, D., Harris, K., and Judkins, J., "Electronic Prognostics System Implementation on Power Actuator Components," *Aerospace Conference, 2008 IEEE*, 2008, pp. 1 – 11.
- <sup>11</sup>Goodman, D., J. H., and J. J., "Electronic prognostics for switched mode power supplies," *Microelectronics Reliability*, Vol. 47(12), 2007, pp. 1902–1906.
- <sup>12</sup>Orsagh, R. and et'al, "Prognostic Health Management for Avionics System Power Supplies," *Aerospace Conference, 2006 IEEE*, March 2006, pp. 1–7.
- <sup>13</sup>Nie, L., Azarian, M., Keimasi, M., and Pecht, M., "Prognostics of ceramic capacitor temperature humidity bias reliability using mahalanobis distance," *Circuit World*, Vol. 33(3), 2007, pp. 21 – 28.
- <sup>14</sup>Gu, J., Azarian, M. H., and Pecht, M. G., "Failure Prognostics of Multilayer Ceramic Capacitors in Temperature-Humidity-Bias Conditions," *International Conference on Prognostics and Health Management*, 2008.
- <sup>15</sup>Gu, J. and Pecht, M., "Prognostics and Health Management Using Physics-of-Failure," *54th Annual Reliability and Maintainability Symposium (RAMS)*, 2008.

- <sup>16</sup>Kulkarni, C., Biswas, G., and Koutsoukos, X., "A prognosis case study for electrolytic capacitor degradation in DC-DC converters," *Proceedings of Annual Conference of the PHM Society, September 27 October 1, San Diego, CA, 2009*.
- <sup>17</sup>Celaya, J., Kulkarni, C., Biswas, G., and Goebel, K., "Towards Prognostic of Electrolytic Capacitors," *American Institute of Aeronautics and Astronautics, AIAA Infotech@Aerospace 2011, March 2011, St. Louis, Missouri, 2011*.
- <sup>18</sup>Kulkarni, C., Celaya, J., Biswas, G., and Goebel, K., "Prognostic Modeling and Experimental Techniques for Electrolytic Capacitor Health Monitoring," *The 8th International Workshop on Structural Health Monitoring 2011 (IWSHM) , September 13-15, Stanford University, Stanford, CA, 2011*.
- <sup>19</sup>Celaya, J., Kulkarni, C., Biswas, G., and Goebel, K., "A Model-based Prognostics Methodology for Electrolytic Capacitors Based on Electrical Overstress Accelerated Aging," *Proceedings of Annual Conference of the PHM Society, September 25-29, Montreal, Canada, 2011*.
- <sup>20</sup>Fife, J., "Wet Electrolytic Capacitors," Patent No: 7,099 1, AVX Corporation, Myrtle Beach, SC, Aug 2006.
- <sup>21</sup>MIL-C-62F, "General Specification For Capacitors," *Fixed Electrolytic*, 2008.
- <sup>22</sup>Lahyani, A., Venet, P., Grellet, G., and Viverge, P., "Failure prediction of electrolytic capacitors during operation of a switchmode power supply," *IEEE Transactions on Power Electronics*, Vol. 13, Nov 1998, pp. 1199–1207.
- <sup>23</sup>Eliasson, L., "Aluminium Electrolytic Capacitor's performance in Very High Ripple Current and Temperature Applications," *CARTS Europe 2007 Symposium, Spain, October - November 2007*.
- <sup>24</sup>Chen, *Ripple Current Confusion*, KEME Electronic Corporation, 2004.
- <sup>25</sup>Bengt, A., "Electrolytic Capacitors Theory and Applications," *RIFA Electrolytic Capacitors*, 1995.
- <sup>26</sup>Luo, J., Namburu, M., Pattipati, K., and et'al, "Model-based Prognostic Techniques," *AUTOTESTCON 2003. IEEE Systems Readiness Technology Conference. Proceedings*, Sep 2003, pp. 330– 340.
- <sup>27</sup>Tye, R. P., *Thermal Conductivity*, Academic Press Inc, Burlington, MA, 1968.
- <sup>28</sup>Wit, H. D. and Crevecoeur, C., "The dielectric breakdown of anodic aluminum oxide," *Physics Letters A*, Vol. Volume 50, Issue 5, 1974, pp. 365 – 366.
- <sup>29</sup>Kulkarni, C., Celaya, J., Biswas, G., and Goebel, K., "Prognostic and Experimental Techniques for Electrolytic Capacitor Health Monitoring," *The Annual Reliability and Maintainability Symposium (RAMS), January 23-36, Reno, Nevada., 2012*.
- <sup>30</sup>Rusdi, M., Moroi, Y., Nakahara, H., and Shibata, O., "Evaporation from Water Ethylene Glycol Liquid Mixture," *Langmuir - American Chemical Society*, Vol. 21 (16), 2005, pp. 7308 – 7310.
- <sup>31</sup>Roederstein, V., "Aluminum Capacitors - General Information," *Document - 25001 January 2007, 2007*.
- <sup>32</sup>Kulkarni, C., Biswas, G., Celaya, J., and Goebel, K., "A Case Study for Capacitor Prognostics under Accelerated Degradation," *IEEE 2011 Workshop on Accelerated Stress Testing & Reliability (ASTR), September 28-30, San Francisco, CA, 2011*.
- <sup>33</sup>60068-1, I., "Environmental testing, Part 1: General and guidance," *IEC Standards*, 1988.
- <sup>34</sup>Biologic, *Application note 14-Zfit and equivalent electrical circuits*, BioLogic Science Instruments, 2010.
- <sup>35</sup>Saha, B. and Goebel, K., "Modeling Li-ion battery capacity depletion in a particle filtering framework," *Proceedings of the Annual Conference of the Prognostics and Health Management Society 2009*, Sept. 2009.
- <sup>36</sup>Daigle, M., Saha, B., and Goebel, K., "A Comparison of Filter-based Approaches for Model-based Prognostics," *Proceedings of the 2012 IEEE Aerospace Conference*, March 2012.
- <sup>37</sup>Orchard, M. E., *A particle filtering-based framework for on-line fault diagnosis and failure prognosis*, Ph.D. thesis, Georgia Institute of Technology, 2007.
- <sup>38</sup>Stengel, R., *Optimal Control and Estimation*, Dover Books on Advanced Mathematics, 1994.
- <sup>39</sup>Chatfield, C., *The Analysis of Time Series: An Introduction*, Chapman & Hall/CRC, 2003.
- <sup>40</sup>Saxena, A., Celaya, J., Saha, B., Saha, S., and Goebel, K., "On Applying the Prognostic Performance Metrics," *Annual Conference of the Prognostics and Health Management Society*, Sep 2009.
- <sup>41</sup>Saxena, A., Celaya, J., Balaban, E., Goebel, K., Saha, B., Saha, S., and Schwabacher, M., "Metrics for evaluating performance of prognostic techniques," *International Conference on Prognostics and Health Management 2008*, 2008.